Drug Design, Development and Therapy

Dovepress

open access to scientific and medical research

Open Access Full Text Article

ORIGINAL RESEARCH

Investigating the Impact of SN-38 on Mouse Brain Metabolism Based on Metabolomics

Xiaodong Zhu[1], Ya Huang[2], Jia Ding[1], Jianguo Liu[1], Changmeng Cui[1], Guangkui Han[1]

[1]Department of Neurosurgery, Affiliated Hospital of Jining Medical University, Jining, 272000, People's Republic of China; [2]College of Traditional Chinese Medicine, Shandong Polytechnic College, Jining, 272000, People's Republic of China

Correspondence: Guangkui Han, Department of Neurosurgery, Affiliated Hospital of Jining Medical University, 89 Guhuai Road, Jining, Shandong, 272000, People's Republic of China, Tel +8618266808351, Email hanguangkui1997@163.com

Purpose: SN-38 (7-ethyl-10-hydroxycamptothecin), the active metabolite of irinotecan, has been extensively studied in drug delivery systems. However, its impact on neural metabolism remains unclear. This study aims to investigate the toxic effects of SN-38 on mouse brain metabolism.

Methods: Male mice were divided into an SN-38 group and a control group. The SN-38 group received SN-38 (20 mg/kg/day) via intraperitoneal injection, while the control group was given an equal volume of a blank solvent mixture (DMSO and saline, ratio 1:9). Gas chromatography-mass spectrometry (GC-MS) was employed to analyze differential metabolites in the cortical and hippocampal regions of the SN-38-treated mice.

Results: SN-38 induced metabolic disturbances in the central nervous system. Eighteen differential metabolites were identified in the hippocampus and twenty-four in the cortex, with six common to both regions. KEGG pathway enrichment analysis revealed statistically significant alterations in six metabolic pathways in the hippocampus and ten in the cortex ($P<0.05$).

Conclusion: This study is the first to demonstrate the neurotoxicity of SN-38 in male mice through metabolomics. Differential metabolites in the hippocampal and cortical regions were closely linked to purine metabolism, pyrimidine metabolism, amino acid metabolism, and glyceride metabolism, indicating disruptions in the blood-brain barrier, energy metabolism, and central signaling pathways.

Keywords: SN-38 (7-ethyl-10-hydroxycamptothecin), biomarker, gas chromatography mass spectrometry, metabolomics, toxicity mechanism

Introduction

Ethyl-10-hydroxycamptothecin (SN-38) is the active metabolite of irinotecan (camptothecin-11, also known as hydrochloride irinotecan). Irinotecan, a broad-spectrum cytotoxic anticancer drug, is widely used to treat various solid tumors and is frequently combined with other chemotherapeutic agents in treating cancers of the central nervous system (CNS). SN-38's antitumor activity is 100 to 1000 times more potent than CPT-11, leading to its extensive study in various drug delivery and controlled release systems.[1] Several SN38 prodrugs, including DTS108, EZN-2208, and SN38 antibody-drug conjugates (ADCs) such as IMMU132 and IMMU130, are currently in clinical trials.[2] Previously, our team developed an effective antitumor drug release system, the SN-38 loaded PCL/GT electrospun film, and investigated its cytotoxicity against gliomas.[3]

The central mechanism of SN-38's anti-tumor activity involves inhibiting DNA topoisomerase I, resulting in DNA damage and cell death in rapidly proliferating normal cells, including bone marrow and intestinal basal cells. Studies have reported common hematologic and gastrointestinal side effects in cancer patients treated with Irinotecan.[4] Rarer toxicities, including articulatory disorders, severe systemic weakness, paralysis, and aphasia induced by irinotecan, have also been reported.[5] However, research on SN-38's effects on brain tissue is limited. Thus, the aim of this experiment is to thoroughly evaluate the neurotoxicity of SN-38 by examining its metabolite levels in the hippocampus and cerebral cortex, and to initially explore the specific mechanisms of SN-38-induced toxicity.

Received: 3 January 2024
Accepted: 14 June 2024
Published: 20 June 2024

Metabolomics plays a crucial role in the realm of systems biology. By combining it with other omics data such as genomics, transcriptomics, and proteomics, a more holistic molecular profile is achieved. This amalgamation offers a deeper understanding of various states such as disease pathology, pharmacological impacts, and responses to stress, while revealing underlying molecular processes. The use of multi-omics integration is prevalent across various domains, encompassing fundamental medical science, clinical diagnostics, pharmaceutical innovation, agricultural enhancement, and research into stress tolerance.[6–8]

Building on neurotissue engineering research, our team employed an established metabolomics research platform to determine the overall impact of SN-38 on brain metabolites and metabolic pathways. This approach clarified the metabolic profile following SN-38 exposure and offered experimental evidence for clinical translation.

Materials and Methods

Chemicals and Reagents

SN-38 was obtained from MedChemExpress, Shanghai, China. Dimethyl sulfoxide (DMSO) was obtained from Tianjin Yongda Chemical Reagents, Tianjin, China. Heptadecanoic acid (purity 98%), methanol (chromatographic grade), and pyridine were obtained from Shanghai Macklin Biochemical, Shanghai, China. O-methylhydroxylamine hydrochloride (purity 98%) was purchased from J&K Scientific Ltd., Beijing, China. N, O-bis(trimethylsilyl)trifluoroacetamide (containing 1% trimethylchlorosilane) was obtained from Sigma Aldrich, St. Louis, MO, USA. Purified water was purchased from Hangzhou Wahaha Company, Hangzhou, China.

Animal Treatment

In this research, 20 male Kunming mice, 6 weeks old, were procured from Jinan Pengyue Experimental Animal Breeding Co., Ltd., based in Jinan, China. Using male mice minimizes hormone-related variability, eliminating confounding factors like estrous cycles.[9] These mice were housed at a steady temperature of 22±2°C and a humidity range of 60–70%, with a 12-hour light/dark cycle maintained. They had free access to standard food and water throughout the study. A week-long adaptation period was observed before initiating the main experiment. To determine the appropriate sample size, we used the Resource Equation Method. The mice were then evenly divided into a control group and a test group, each containing 10 mice. For the experimental procedure, SN-38 was mixed in a solution of sodium chloride and 5% DMSO to achieve the required concentrations. The test group (n=10) received daily intraperitoneal injections of SN-38 (20 mg/kg) for a week. The drug schedule was established based on existing research.[10] The control group, consisting of 10 mice, was administered an equivalent volume of a blank solvent mixture (DMSO and saline in a 1:9 ratio). This study was performed in accordance with the Laboratory animal—Guideline for ethical review of animal welfare of China (GB/T 35892–2018) and approved by the Ethics Committee of the Affiliated Hospital of Jining Medical University (Approval Number: JNMC-2022-DW-041).

Sample Collection and Preparation

The mice were euthanized on the second day following the final dose. Initially, 0.1 mg/kg of Atropine sulfate is administered intraperitoneally, followed by anesthesia using a 10% solution of chloral hydrate to achieve both hypnotic and analgesic effects. Animals are subsequently euthanized using cervical dislocation. Subsequently, the cerebral cortex and hippocampus tissues were promptly removed, immediately cooled on ice, rinsed with phosphate-buffered saline at pH 7.2, rapidly frozen in liquid nitrogen, and preserved at −80°C. In the tissue processing phase, each 50 mg of tissue was thoroughly homogenized in 1 mL of methanol inside a grinding tube. To this mixture, 50 μL of heptadecanoic acid (concentration 1 mg/mL in methanol) was added, and the mixture was then centrifuged at 4°C for 15 minutes at 14,000 rpm. Following this, 80 μL of O-methylhydroxylamine hydrochloride (15 mg/mL dissolved in pyridine) was introduced to the sample. This was followed by an incubation period at 70°C for 90 minutes, after which 100 μL of N, O-bis(trimethylsilyl)trifluoroacetamide (with 1% trimethylchlorosilane) was added, and the mixture was re-incubated at 70°C for another 60 minutes. A 0.22-μm filter was utilized for the final purification step. Take 10 μL from each sample in both the control and SN-38 groups to use as quality control (QC).

GC-MS Analyses

The analysis of the samples was conducted using an Agilent 7890B GC System coupled with a 7000C Triple Quadrupole Mass Spectrometer, originating from the United States. To maintain consistency and reliability of the instrument, a quality control sample was run after every ten test samples. The samples were injected in a randomized order and underwent separation in an HP-5MS fused silica capillary column. Helium was employed as the carrier gas, with a split ratio of 50:1. The settings for the front inlet purge flow were at 3 mL/min, while the overall gas flow rate was maintained at 1 mL/min. The transfer line, sample inlet, and ion source temperatures were set at 250°C, 280°C, and 230°C, respectively. The GC's temperature protocol commenced at 60°C, held for 4 minutes, followed by an increment of 8°C per minute up to 300°C, where it remained for 5 minutes. The electron beam energy was calibrated to −70eV, and the system recorded data at a rate of 20 spectra per second. For mass spectrometry, electrospray ionization was utilized, scanning a full mass-to-charge (m/z) range from 50 to 800.

Data Processing and Metabolite Identification

The acquired data from Gas Chromatography-Mass Spectrometry (GC-MS) underwent analysis using the Agilent Mass Hunter software, Version B.07.00, from Agilent Technologies, based in California, USA. This process involved converting the raw data into a mass-to-charge ratio (m/z) format. The study categorized metabolites as Level 2, representing putatively annotated compounds, determined by their resemblance to existing commercial spectral libraries.[11] A comprehensive spectral library, encompassing all quality control samples, was compiled. The National Institute of Standards and Technology (NIST 14) GC-MS library from the United States played a pivotal role in identifying unknown metabolites. This included procedures like alignment, time correction, baseline filtering, and deconvolution. Metabolites with a structural identification similarity exceeding 80% underwent manual verification to ensure precision. Subsequently, a bespoke spectral library was constructed for matching the experimental samples, culminating in a unified data matrix containing peak indices (RT-m/z pairs), sample identifiers, and corresponding peak areas.

Normalization of these peak areas within the data matrix was executed using Microsoft Excel™, from Microsoft, Redmond, WA, USA. The three-dimensional dataset, consisting of peak indices (RT-m/z pairs), sample names, and normalized peak area percentages, was imported into SIMCA-P 14.0 (Umetrics, Umeå, Sweden) for statistical analysis. Unsupervised Principal Component Analysis (PCA) and Orthogonal Projections to Latent Structures Discriminant Analysis (OPLS-DA) were used to distinguish between the SN-38-treated group and the control group. The validity of the model was confirmed using a permutation test with SIMCA-P software. A two-tailed Student's *t*-test was conducted using SPSS 19.0 (SPSS Inc, Chicago, IL, USA). In the OPLS-DA, variables with Importance in Projection (VIP) values greater than 1.0 and p-values less than 0.05 were deemed statistically significant and selected for identifying differential metabolites.

Statistical Analysis

We rigorously assessed the data distribution and homogeneity using IBM SPSS Statistics 19.We applied the Shapiro–Wilk test for normality, selecting compounds with significance (Sig) values greater than 0.05 in both sample groups. Levene's Test assessed the homogeneity of variance, selecting compounds with a mean Sig value greater than 0.05. Compounds that met both criteria underwent further analysis. We used the Independent-Samples *T* Test for parametric data to identify significant compounds based on specific Sig values, and the Mann–Whitney *U*-Test for non-parametric data. These steps ensured that our data met the necessary assumptions for valid statistical testing, enhancing the robustness and reliability of our findings.

Metabolic Pathway Analysis

For the pathway analysis in this study, MetaboAnalyst 6.0 (available at http://www.metaboanalyst.ca) and the Kyoto Encyclopedia of Genes and Genomes (KEGG; accessible at http://www.kegg.jp) were employed. Key discriminant metabolites were pinpointed based on having variable importance in projection (VIP) values exceeding 1.0 and two-

tailed Student's *t*-test p-values falling below 0.05. These selected metabolites underwent further examination through pathway analysis tools, aiming to pinpoint differential metabolites and their significant metabolic pathways. Pathways that exhibited a raw p-value less than 0.05 were deemed significant in the context of SN-38 toxicity.

Results

GC-MS TICs

Figure 1 displays the total ion chromatograms (TICs) of quality control samples derived from both cortical and hippocampal tissues. These chromatograms reveal the successful detection of various metabolites throughout the run time, characterized by substantial peak capacities, consistent retention times, and outstanding reproducibility.

Multivariate Analysis of Metabolomic Data

Table 1 provides a detailed description of the OPLS-DA model parameters, each approaching a value close to 1.0. The model's robustness is evidenced by a ranking test, which confirms its reliability; all intersection points of the blue regression line (Q2-points) with the left vertical axis are negative (Figure 2). Furthermore, the OPLS-DA analysis distinctly demonstrates a significant difference between the SN-38 and control groups.

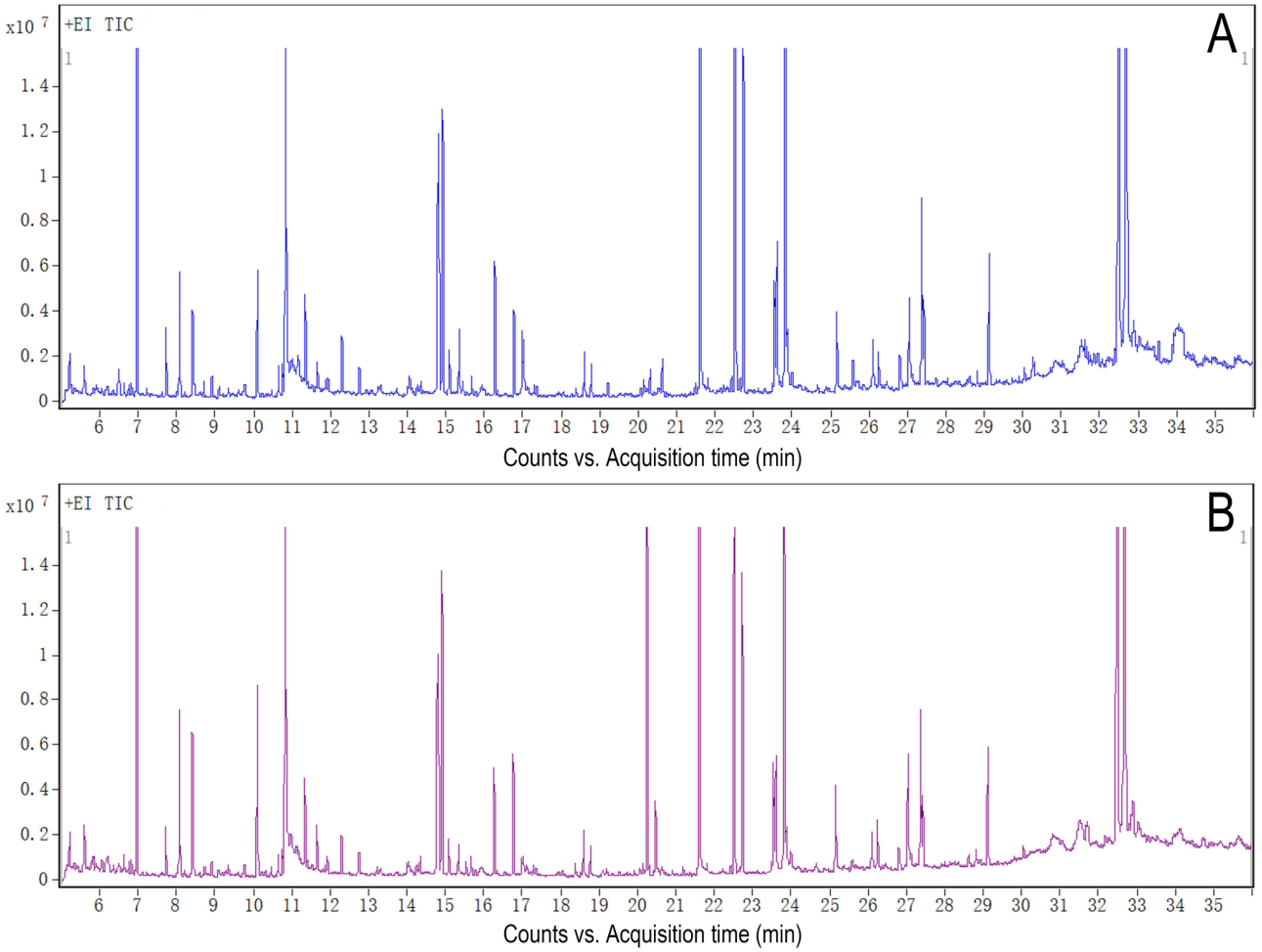

Figure 1 Representative gas chromatography–mass spectrometry (GC–MS) total ion chromatograms (TICs) from quality control (QC) samples. (**A**) the hippopotamus and (**B**) the the cerebral cortex.

Table 1 The Scores of the Model Parameters

	R^2X(cum)	R^2Y(cum)	Q^2(cum)
Hippocampus	0.392	0.988	0.648
Cerebral cortex	0.407	0.994	0.828

Identification of Metabolic Changes

Metabolite identification was based on a well-established mass spectrometry database, initially using the Agilent Fiehn GC/MS Metabolomics RTL Library for profile comparison.Standard criteria for metabolite identification include VIP scores and p-values.Metabolites are marked as significantly altered between groups if they have a VIP score over 1 in OPLS-DA analysis and a p-value under 0.05 in the Student's *t*-test.Table 2 outlines altered metabolites in tissues across groups.Post-SN-38 challenge, the hippocampus showed 2 increased and 16 decreased metabolites compared to the control group.SN-38 exposure in the cerebral cortex resulted in 24 altered metabolites: 3 up-regulated and 21 down-regulated.Heatmaps are used for quality control and to present differential data.Clustering groups similar items into categories or subsets through static classification, highlighting similarities within each subset.Figure 3 illustrates significant group differences.

Analyses of Metabolic Pathways

MetaboAnalyst 6.0 was used to analyze identified metabolites and assess metabolic alterations between the SN-38 and control groups. Metabolic pathways with a Raw P-value < 0.05 (see Table 3 and Figure 4) were deemed potentially disturbed. Figure 5 presents a detailed metabolic network diagram. The Results indicated that SN-38 exposure affected multiple metabolic pathways, including those for various amino acids, propanoate, purine, pyrimidine, butanoate, glyoxylate, and dicarboxylate, as well as glycerolipid metabolism. Additionally, pathways involved in pantothenate and CoA biosynthesis and the biosynthesis of unsaturated fatty acids were also impacted.

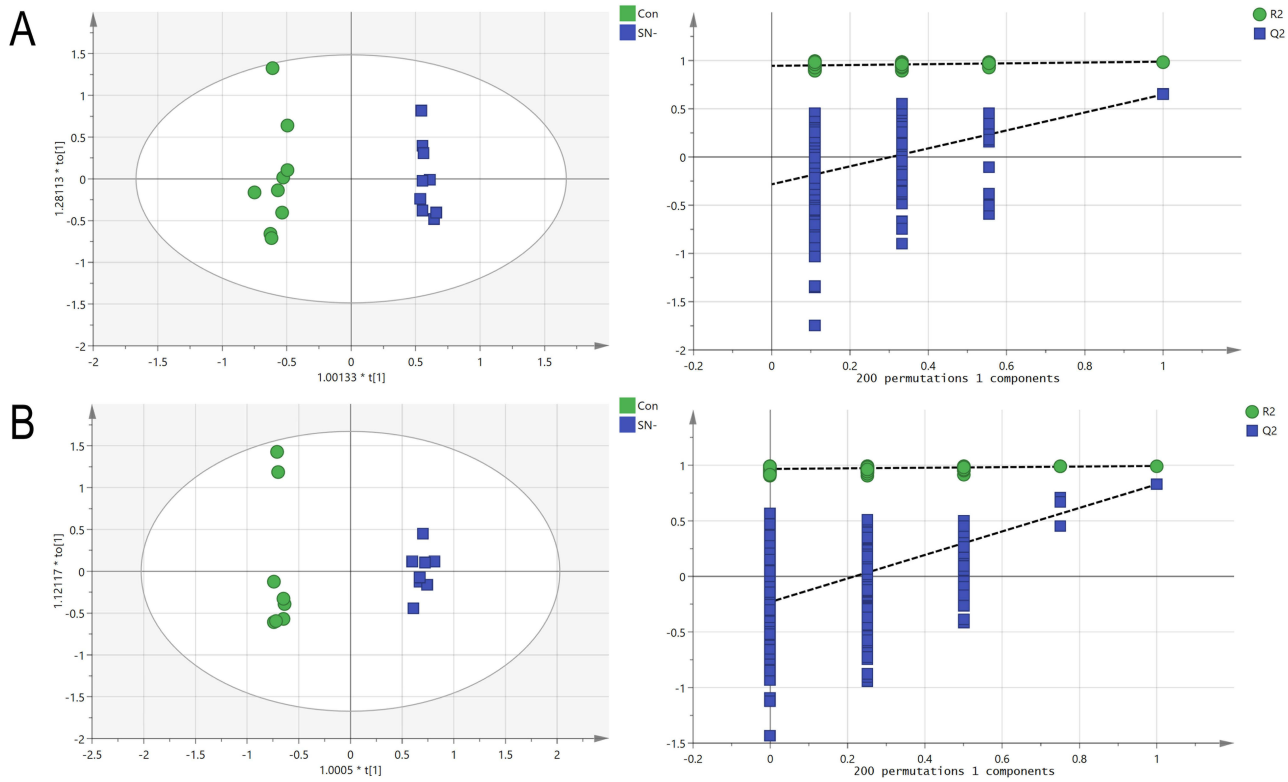

Figure 2 OPLS-DA score plots and permutation tests. (**A**)Hippocampus (**B**) Cerebral cortex.

Discussion

Clinical evidence indicates that the toxic effects of Irinotecan and its metabolite SN-38 are primarily manifested in the gastrointestinal tract and liver, with little reported toxicity to other organs. For the first time, we evaluated the nervous system in mice, employing multivariate statistical analysis to study the neurotoxicity related to SN-38 and potential biomarkers. This could aid researchers in understanding the pathogenesis of SN-38-induced neurotoxicity. In our study, 36 potential biomarkers were identified, 18 in the hippocampus and 24 in the cortex; these will be discussed separately below.

Adenosine not only participates in ATP formation but also serves as a signaling molecule in purinergic pathways. In the central nervous system(CNS), purinergic receptors are prevalent in neurons, glial cells, and vascular endothelial cells.[12,13] This signaling is instrumental in maintaining the functionality and homeostasis of neuronal, astrocytic, and microglial cells, thereby facilitating essential processes such as synaptic transmission and higher cognitive functions[14–16] Recent studies highlight purinergic signaling's role in modulating blood-brain barrier permeability.[17,18] Pathway analysis reveals disrupted purine metabolism in the hippocampus of the SN-38 group, accompanied by an increased adenosine level in the cortex. This indicates blood-brain barrier dysfunction and energy metabolic disorders. Purine metabolism dysregulation is a known factor in the pathogenesis of neurodegenerative diseases, including Alzheimer's and Parkinson's disease,[19,20] pointing to potential signaling pathway and cognitive function disruptions due to SN-38 treatment.

Table 2 Differential Metabolites in Different Tissues After SN-38 Treatment

Samples	Metabolites	HMDB ID	VIP	p-value	Fold change
Hippocampus	N-Dodecane	HMDB0031444	0.935179	0.022	0.779712
	L-Alanine	HMDB0000161	1.2432	0.001	0.780999
	Beta-Alanine	HMDB0000056	1.24455	0.004	0.763298
	Oxalic acid	HMDB0002329	1.09233	0.019	0.781427
	O-Phosphoethanolamine	HMDB0000224	1.85869	0	0.590684
	L-Tyrosine	HMDB0000158	1.42048	0	0.741043
	scyllo-Inositol	HMDB0006088	1.49664	0	0.726179
	Ribothymidine	HMDB0000884	1.05567	0.016	1.23005
	Arachidic acid	HMDB0002212	1.20825	0.019	0.747809
	Uridine	HMDB0000296	1.1302	0.007	1.22134
	Inosine	HMDB0000195	1.06666	0.003	0.813259
	Guanosine	HMDB0000133	2.16882	0.001	0.483594
	Cholesterol	HMDB0000067	1.1387	0.026	0.762898
	L-Lactic acid	HMDB0000190	2.00912	0	0.591114
	Urea	HMDB0000294	1.09792	0.031	0.788596
	Succinic acid	HMDB0000254	2.97199	0.019	0.142377
	Oleic acid	HMDB0000207	1.10526	0.024	0.722348
	2,5-Furandicarboxylic acid	HMDB0004812	1.522	0	0.715994

(*Continued*)

Table 2 (Continued).

Samples	Metabolites	HMDB ID	VIP	p-value	Fold change
Cerebral cortex	D-Lactic acid	HMDB0001311	1.45558	0	0.646974
	L-Alanine	HMDB0000161	1.25143	0.002	0.720946
	L-Valine	HMDB0000883	1.61827	0	0.628527
	Glycerol	HMDB0000131	1.04313	0	0.812167
	Gamma-Aminobutyric acid	HMDB0000112	1.63792	0	0.637064
	Glyceric acid	HMDB0000139	1.16445	0.047	0.668106
	Uracil	HMDB0000300	1.44232	0	0.678135
	Serine	HMDB0062263	1.42756	0	0.699546
	L-Threonine	HMDB0000167	1.25731	0.001	0.724564
	L-Aspartic acid	HMDB0000191	1.19529	0	0.757575
	Beta-Alanine	HMDB0000056	2.28132	0	0.411832
	L-Glutamic acid	HMDB0000148	1.2445	0.002	1.38101
	Taurine	HMDB0000251	1.02676	0.032	0.712355
	O-Phosphoethanolamine	HMDB0000224	2.67578	0	0.283213
	L-Lysine	HMDB0000182	1.64567	0	0.617583
	scyllo-Inositol	HMDB0006088	1.38441	0.045	0.593565
	Inosine	HMDB0000195	1.24768	0	1.32621
	Glycine	HMDB0000123	1.10208	0.01	0.741338
	Ethanolamine	HMDB0000149	1.99027	0	0.533868
	L-Isoleucine	HMDB0000172	1.60849	0	0.631164
	Hypoxanthine	HMDB0000157	1.67037	0	0.640728
	Citric acid	HMDB0000094	1.88007	0	0.521356
	L-Tyrosine	HMDB0000158	1.38276	0.01	0.605454
	Adenosine	HMDB0000050	2.80038	0	8.10382

Guanosine, a purine nucleoside, exhibits neuroprotective effects in conditions like ischemic stroke, Alzheimer's disease, and Parkinson's disease.[21–23] Its neuroprotection involves multiple mechanisms: reducing glutamatergic excitotoxicity in astrocytes,[24] modulating the adenosinergic system,[25] and affecting inflammatory cascades and oxidative stress.[26] This study's finding of reduced guanosine in the hippocampus implies a compromised neuroprotection in the SN-38 group.

Amino acids and their metabolites regulate neuronal activity in the CNS, assisting in diagnosing various diseases.[27] In comparison to the control group, the SN-38 group exhibited a downregulation of L-alanine, L-tyrosine, valine, serine, L-threonine, L-aspartate, L-lysine, glycine, and L-isoleucine, as well as an upregulation of L-glutamate. The affected metabolic pathways include alanine, aspartate, and glutamate metabolism; arginine biosynthesis; and biosynthesis of phenylalanine, tyrosine, and tryptophan; as well as valine, leucine, and isoleucine; glycine, serine, and threonine; and histidine metabolism. Glutamate, an excitatory neurotransmitter, is crucial in cellular metabolism and implicated in

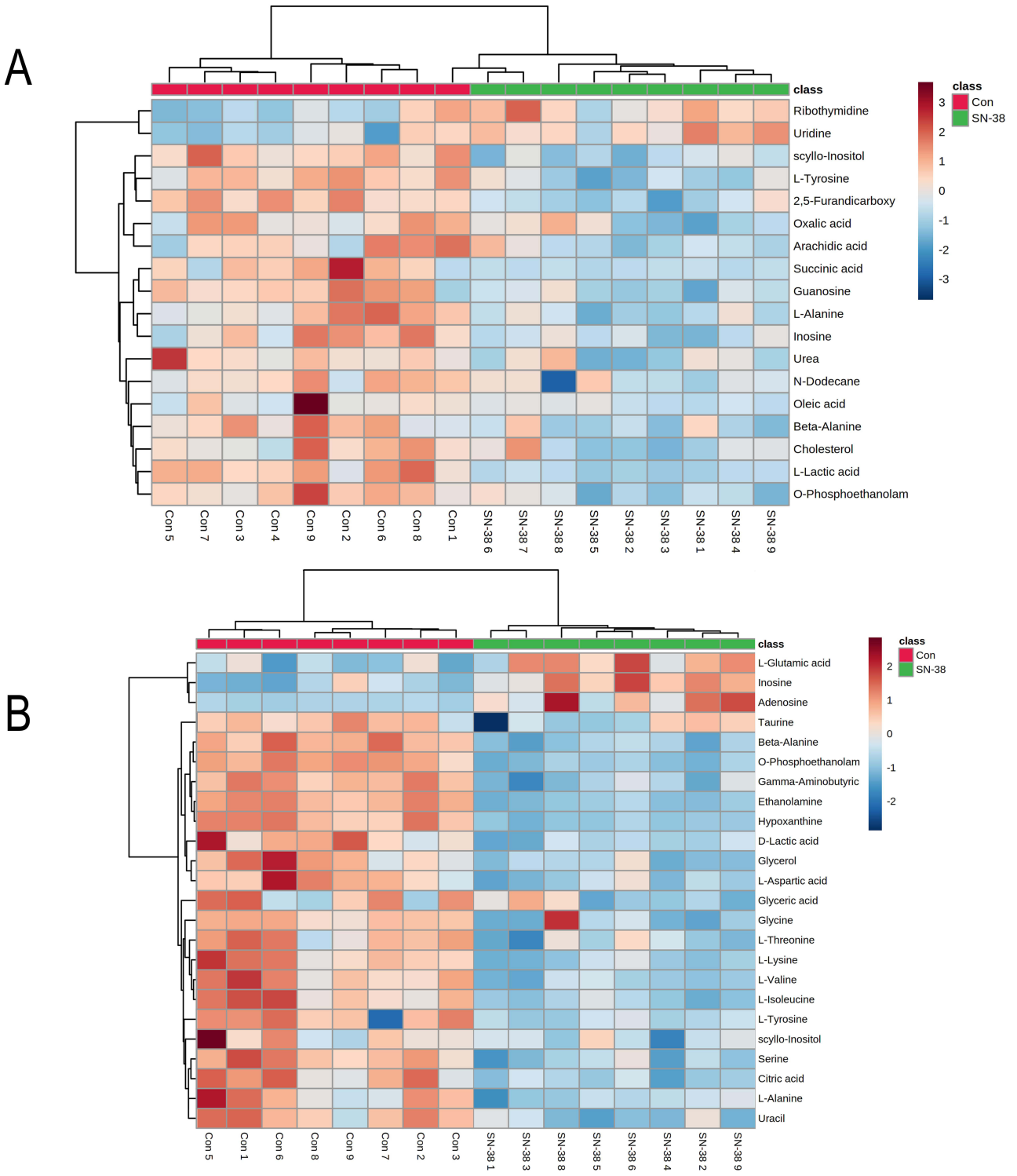

Figure 3 Heatmap of differential metabolites in the SN-38 group compared with controls, featuring: (**A**) Hippocampus and (**B**) Cerebral Cortex.Each color in the heatmap represents metabolite changes: blue for down-regulation, and red for up-regulation.In the heatmap, rows represent samples and columns represent metabolites.

neuropsychiatric disorders such as epilepsy, schizophrenia, and depression. Stress and inflammation may increase glutamate, further harming neurons. Brain endothelial cells exposed to high levels of glutamate activate N-methyl-D-aspartate receptors, disrupting the blood-brain barrier.[28] Aspartate, a non-essential amino acid, exhibits abnormal levels in various neurological disorders.[29] It affects glycolysis via the malate-aspartate shuttle, disrupting brain energy

Table 3 Pathway Analysis Performed Using MetaboAnalyst 6.0 Software

Samples	Pathway Names	Raw p	Impact
Hippocampus	Propanoate metabolism	0.014045	0.0
	Purine metabolism	0.019694	0.00274
	Alanine, aspartate and glutamate metabolism	0.022329	0.0
	Phenylalanine, tyrosine and tryptophan biosynthesis	0.033654	0.5
	Biosynthesis of unsaturated fatty acids	0.035813	0.0
	Pyrimidine metabolism	0.041522	0.03985
Cerebral cortex	Alanine, aspartate and glutamate metabolism	3.83E-05	0.50722
	Glyoxylate and dicarboxylate metabolism	7.54E-05	0.25927
	Valine, leucine and isoleucine biosynthesis	0.00015938	0
	Pantothenate and CoA biosynthesis	0.00016191	0.04762
	Glycine, serine and threonine metabolism	0.0013463	0.53603
	beta-Alanine metabolism	0.0033292	0.39925
	Arginine biosynthesis	0.017698	0.11675
	Butanoate metabolism	0.020234	0.03175
	Histidine metabolism	0.022915	0
	Glycerolipid metabolism	0.022915	0.33022

Abbreviations:SN-38, Ethyl-10-hydroxycamptothecin;TICs, total ion chromatograms; GC-MS, Gas Chromatography-Mass Spectrometry;CNS, central nervous system;ATP, Adenosine 5'-triphosphate;GABA, γ-aminobutyric acid;BCAAs, Branched-chain amino acids;TAG, triacylglycerol;PE, phosphatidylethanolamine.

metabolism.[30] Aspartate also regulates nitrogen and carbon dioxide levels in the blood and offers neuroprotection.[31] Glutamate's metabolism into γ-aminobutyric acid(GABA) through butyrate metabolism makes it the CNS's primary inhibitory neurotransmitter. Reduced GABA levels are linked to increased neuronal excitability and cognitive impairments. Studies show reduced GABA in Alzheimer's patients.[32]

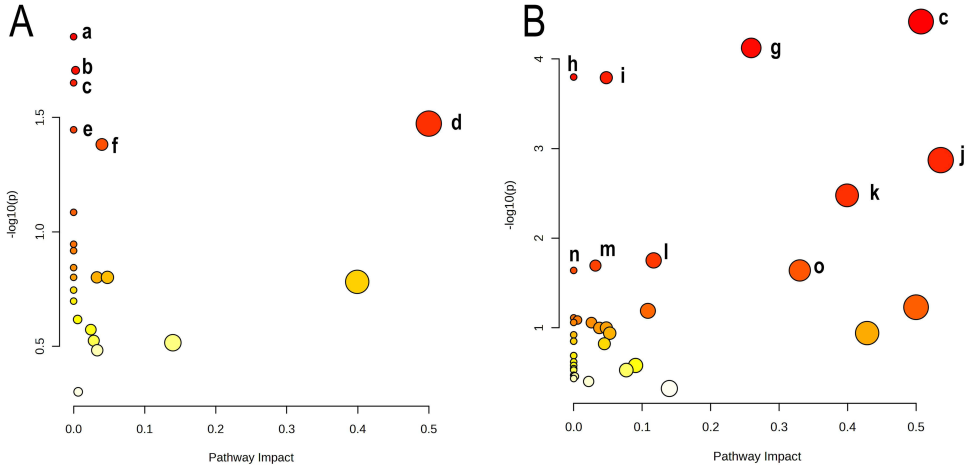

Figure 4 Summary of the pathway analysis conducted with MetaboAnalyst 6.0. The metabolome view shows all matched pathways according to the p values from the pathway enrichment analysis and pathway impact values from the pathway topology analysis. (**A**)Hippocampus: a Propanoate metabolism; b Purine metabolism; c Alanine, aspartate and glutamate metabolism; d Phenylalanine, tyrosine and tryptophan biosynthesis; e Biosynthesis of unsaturated fatty acids; f Pyrimidine metabolism; (**B**) Cerebral cortex: c Alanine, aspartate and glutamate metabolism; g Glyoxylate and dicarboxylate metabolism; h Valine, leucine and isoleucine biosynthesis; i Pantothenate and CoA biosynthesis; j Glycine, serine and threonine metabolism; k beta-Alanine metabolism; l Arginine biosynthesis; m Butanoate metabolism; n Histidine metabolism; o Glycerolipid metabolism.

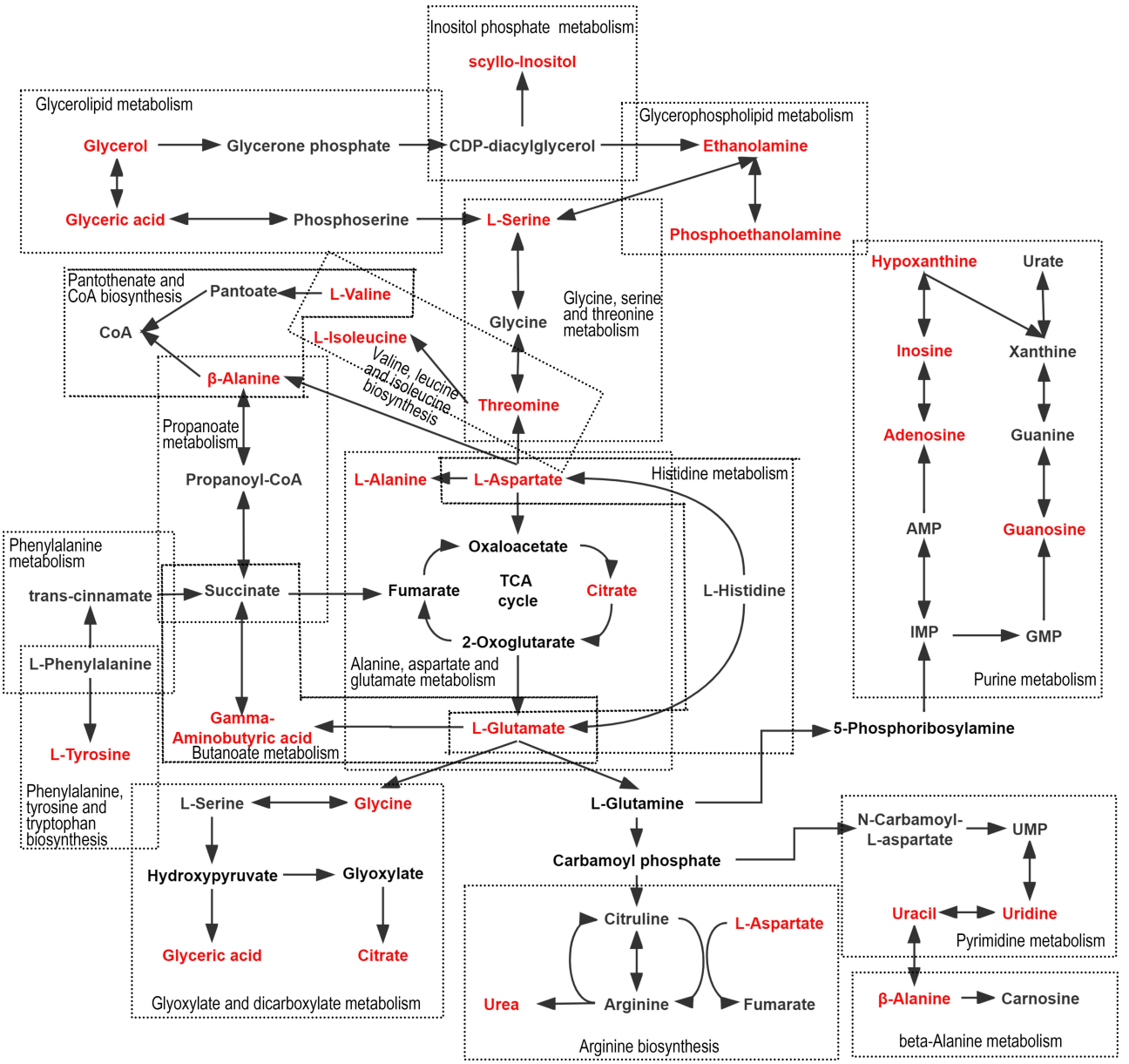

Figure 5 Schematic diagram showing metabolic pathways in tissues affected by SN-38 processing.Metabolites marked in red indicate potential biomarkers identified in this study.

Branched-chain amino acids(BCAAs), key metabolic precursors, play a role in neurotransmitter synthesis and amino acid metabolism in the brain.[33] Studies show reduced valine and isoleucine levels in the cortical tissue of SN-38-treated mice compared to controls, indicating an effect on BCAA biosynthesis. This suggests that SN-38 could negatively impact brain function by disrupting the synthesis of vital proteins, neurotransmitters, and metabolites. Tyrosine, a catecholamine precursor, influences neural transmission through its varying levels.[34] Histidine, a carnosine precursor, contributes to carnosine synthesis, utilizing ATP hydrolysis and β-alanine. Carnosine functions significantly as a buffer and antioxidant.[35] Animal research reveals β-alanine supplementation enhances brain carnosine levels, offering neuroprotection.[36] While human studies have not shown a significant increase in brain carnosine levels, evidence suggests β-alanine may enhance cognitive function and mood,[37] although the exact mechanisms are still unknown. Research links phenylalanine, tyrosine, and tryptophan biosynthesis to Alzheimer's disease.[38] Overall, amino acid

metabolic alterations in the cortex and hippocampus of SN-38-treated mice could illuminate SN-38-induced neurotoxicity pathogenesis.

Metabolomic and lipidomic analyses revealed abnormal glycerolipid metabolism in the brains of SN-38-treated mice. Glycerol, a crucial energy reserve, stores excess glucose as triglycerides in the body. Research has confirmed that diminished levels of triacylglycerol (TAG) correlate strongly with an increased severity of cognitive impairments, underscoring the critical role of lipid metabolism in brain function. Glycerolipids, significant as signaling molecules in the central nervous system, play key roles in appetite control, immune system regulation, and pain management.[39]

The observed abnormalities in triglyceride metabolism suggest a broader disruption that extends to glycerophospholipid and myo-inositol phosphate metabolism, potentially impacting these critical signaling pathways.The reduction in phosphatidylethanolamine (PE), a major component and precursor in brain phospholipid synthesis, usually indicates compromised myelination and could thus exacerbate cognitive and behavioral deficits.[40] The link between PE and epilepsy is well-documented.[41] Myo-inositol, prevalent in central glial cells, reflects glial cell activity. Studies show elevated brain myo-inositol levels in Alzheimer's, amnestic mild cognitive impairment, and chronic alcoholism patients. Conversely, lower brain myo-inositol levels in fibromyalgia patients correlate with memory and attention deficits.[42] This study's observed changes in PE and myo-inositol levels suggest links to brain dysfunction-related diseases, warranting further investigation.

The metabolomic study results elucidate the effects of SN-38 on brain metabolism. However, the study has limitations; further experiments in animal tumor models are needed to understand the impact of SN-38 on brain metabolism. Based on the established metabolomics platform, the drug-related toxicity of SN-38 in combination with other chemotherapy drugs still requires experimental evaluation. This evaluation can help advance the clinical application of various SN-38 delivery systems. In our research, atropine sulfate combined with chloral hydrate was chosen to anesthetize rats due to its rapid induction of sleep and anticonvulsant properties. Despite its historical use in small animal anesthesia, chloral hydrate has limitations. Increasing evidence suggests that it does not provide sufficient analgesia and can cause significant respiratory depression at doses required for surgical anesthesia, posing potential risks to animal health and experimental safety.[43] Considering these limitations, we plan to replace chloral hydrate with safer anesthetics such as pentobarbital or isoflurane in future studies.

Conclusion

This study employed GC-mass spectrometry to investigate the metabolomic profile of the nervous system in mice exposed to SN-38. Through initial screening of metabolites, 24 and 18 characteristic metabolites were identified in the cortex and hippocampus, respectively. It was found that SN-38 affects purine metabolism, pyrimidine metabolism, amino acid metabolism, and glycerolipid metabolism in the central nervous system, leading to blood-brain barrier disruption, abnormal energy metabolism, and central signaling pathway disorders. This metabolomics data provides new evidence for studying the neurotoxicity induced by SN-38.

Funding

This work was supported by the National Natural Science Foundation of China (Grant No.82302795); Natural Science Foundation of Shandong Province [ZR2023QH094]; Jining Key Research and Development Program [2022YXNS019]; Nursery Research Project of Affiliated Hospital of Jining Medical University [MP-MS-2022-006].

Disclosure

The authors report no conflicts of interest in this work.

References

1. Yang J, Jia L, He Z. et al. Recent advances in SN-38 drug delivery system.*Int. J Pharmaceut*. 2023:637. 10.1016/j.ijpharm.2023.122886.
2. Qi Q, Tian H, Yue B, et al. Research progress of SN38 drug delivery system in cancer treatment. *Int J Nanomed*. 2024;19:945–964. doi:10.2147/IJN.S435407

3. Zhu X, Ni S, Xia T, et al. Anti-neoplastic cytotoxicity of SN-38-loaded PCL/Gelatin electrospun composite nanofiber scaffolds against human glioblastoma cells in vitro. *J Pharm Sci*. 2015;104(12):4345–4354. doi:10.1002/jps.24684
4. Bao X, Wu J, Kim S, et al. Pharmacometabolomics reveals irinotecan mechanism of action in cancer patients. *J Clini Pharma*. 2018;1(1):1–15. doi:10.1002/jcph.1275
5. De Lisa M, Ballatore Z, Marcantognini G, et al. Irinotecan-induced transient dysarthria: case series and updated literature review. *Oncol Ther*. 2020;8(1):147–160. doi:10.1007/s40487-019-00106-z)
6. Gupta N, Vats S, Bhargava P. Sustainable agriculture: role of metagenomics and metabolomics in exploring the soil microbiota, in: silico Approach for Sustainable Agriculture. *Springer*. 2018;183–199. doi:10.1007/978-981-13-0347-0_11
7. Shoaib M, Choudhary R, Choi J, et al. Plasma metabolomics supports the use of long-duration cardiac arrest rodent model to study human disease by demonstrating similar metabolic alterations. *Sci Rep*. 2020; 10(1): 19707. 10.1038/s41598-020-76401-x
8. Pang H, Jia W, Hu Z. Emerging applications of metabolomics in clinical pharmacology. *Clin Pharmacol Ther*. 2019;106(3):544–556. doi:10.1002/cpt.1538
9. Nobre LMS, da Silva Lopes MH, Geraix J, et al. Paraprobiotic Enterococcus faecalis EC-12 prevents the development of irinotecan-induced intestinal mucositis in mice. *Life Sci*. 2022;296:120445. doi:10.1016/j.lfs.2022.120445
10. Takeda M, Koseki J, Takahashi H, et al. Disruption of endolysosomal RAB5/7 efficiently eliminates colorectal cancer stem cells. *Cancer Res*. 2019;79(7):1426–1437. doi:10.1158/0008-5472.CAN-18-2192))
11. Viant MR, Kurland IJ, Jones MR, et al. How close are we to complete annotation of metabolomes?. *Curr Opin Chem Biol*. 2017;36:64–69. doi:10.1016/j.cbpa.2017.01.001
12. Burnstock G. Physiology and pathophysiology of purinergic neurotransmission. *Physiol Rev*. 2007;87(2):659–797. doi:10.1152/physrev.00043.2006
13. Muhleder S, Fuchs C, Basilio J, et al. Purinergic P2Y2 receptors modulate endothelial sprouting. *Cell Mol Life Sci*. 2020;77(5):885–901. doi:10.1007/s00018-019-03213-2
14. Burnstock G. Introduction to purinergic signalling in the brain. *Adv Exp Med Biol*. 1202;1–12. doi:10.1007/978-3-030-30651-9_1
15. Burnstock G. Purinergic signalling and neurological diseases: An update. *CNS Neurol Disord Drug Tar*. 2017;16(3):257–265. doi:10.2174/1871527315666160922104848
16. Illes P, Xu GY, Tang Y. Purinergic signaling in the central nervous system in health and disease. *Neurosci Bull*. 2020;36(11):1239–1241. doi:10.1007/s12264-020-00602-7
17. Chen L, Li L, Zhou C, et al. Adenosine A2A receptor activation reduces brain metastasis via SDF-1/CXCR4 axis and protecting blood-brain barrier. *Molecular Carcinogenesis*. 2020;59(4):390–398. doi:10.1002/mc.23161 *Mol. Carcinog*.2020.
18. Wu ST, Han JR, Yao N, et al. Activation of P2X4 receptor exacerbates acute brain injury after intracerebral hemorrhage. *CNS Neurosci Ther*. 2022;28(7):1008–1018. doi:10.1111/cns.13831
19. Bourke CA. Astrocyte dysfunction following molybdenum associated purine loading could initiate Parkinson's disease with dementia. *NPJ Parkinsons Dis*. 2018;4(1):7. doi:10.1038/s41531-018-0045-5
20. Alonso-Andrés P, Albasanz JL, Ferrer I, Martín M. Purine-related metabolites and their converting enzymes are altered in frontal, parietal and temporal cortex at early stages of Alzheimer's disease pathology. *Brain Pathol*. 2018;28(6):933–946. doi:10.1111/bpa.12592
21. Su C, Elfeki N, Ballerini P, et al. Guanosine improves motor behavior, reduces apoptosis, and stimulates neurogenesis in rats with parkinsonism. *J Neurosci Res*. 2009;87(3):617–625. doi:10.1002/jnr.21883
22. Hansel G, Tonon AC, Guella F, et al. Guanosine protects against cortical focal ischemia. Involvement of inflammatory response. *Mol Neurobiol*. 2015;52(3):1791–1803. doi:10.1007/s12035-014-8978-0
23. Lanznaster D, Mack JM, Coelho V, et al. Guanosine prevents anhedonic-like behavior and impairment in hippocampal glutamate transport following amyloid-β1-40 administration in mice. *Molecular Neurobiology*. 2017;54(7):5482–5496. doi:10.1007/s12035-016-0082-1 *Mol. Neurobiol*.2017.
24. Schmidt AP, Tort AB, Souza DO, Lara DR. Guanosine and its modulatory effects on the glutamatergic system. *Eur Neuropsycho*. 2008;18(8):620–622. doi:10.1016/j.euroneuro.2008.01.007
25. Almeida RF, Comasseto DD, Ramos DB, et al. Guanosine anxiolytic-like effect involves adenosinergic and glutamatergic neurotransmitter systems. *Mol Neurobiol*. 2017;54(1):423–436. doi:10.1007/s12035-015-
26. Kovacs Z, Kekesi KA, Dobolyi A, Lakatos R, Juhasz G. Absence epileptic activity changing effects of non-adenosine nucleoside inosine, guanosine and uridine in Wistar Albino Glaxo Rijswijk rats. *Neuroscience*. 2015;300(0):593–608. doi:10.1016/jneuroscience.2015.05.054
27. Razak M, Begum P, Viswanath B, et al. Multifarious beneficial effect of nonessential amino acid, Glycine: a review. *Oxid Med Cell Longev*. 2017;2017:1–8. doi:10.1155/2017/1716701
28. Jiang H, Zhang Y, Wang Z, et al. Connexin 43: an Interface Connecting neuroinflammation to Depression. *Molecules*. 2023;28(4). doi:10.3390/molecules28041820
29. Zhao S, Zhong H, Geng C, et al. Comprehensive analysis of metabolic changes in rats exposed to acrylamide. *Environ Pollut*. 2021;287(0): 117591. doi:10.16/j.envpol.2021.117591
30. Faria M, Ziv T, Gómez-Canela C, et al. Acrylamide acute neurotoxicity in adult zebrafish. *Sci Rep*. 2018;8(1). doi:10.1038/s41598-018-26343-2
31. Thomas G, Budd Samantha L, Lipton Stuart A. Excitatory amino acid neurotoxicity. *Adv Exp Med Biol*. 2002;513(undefined):3–40. doi:10.1007/978-1-4615-0123-7_1
32. Norman JE, Nuthikattu S, Milenkovic D, et al. Sex modifies the impact of type 2 diabetes mellitus on the murine whole brain metabolome. *Metabolites*. 2023;13(9). doi:10.3390/metabo13091012
33. Lu L-H, Xia Z-X, Guo J-L, et al. Metabolomics analysis reveals perturbations of cerebrocortical metabolic pathways in the Pah enu2 mouse model of phenylketonuria. *CNS Neurosci Ther*. 2020;26(4):486–493. doi:10.1111/cns.13214
34. Zhang L, Wong LR, Wong P, et al. Chronic treatment with baicalein alleviates behavioural disorders and improves cerebral blood flow via reverting metabolic abnormalities in a J20 transgenic mouse model of Alzheimer's disease. *Brain, Behavior, & Immunity - Health*. 2023;28. doi:10.1016/j.bbih.2023.100599
35. Brosnan Margaret E, Brosnan John T. Histidine metabolism and function. *J Nutr*. 2020;150(Suppl 1):2570S–2575S. doi:10.1093/jn/nxaa079
36. Ostfeld I, Hoffman JR. The effect of β-alanine supplementation on performance, cognitive function and resiliency in soldiers. *Nutrients*. 2023;15(4):1039. doi:10.3390/nu15041039

37. Meftahi GH, Jahromi GP. Biochemical mechanisms of beneficial effects of beta-alanine supplements on cognition. *Biochemistry*. 2023;88(8). doi:10.1134/S0006297923080114
38. Dejakaisaya H, Harutyunyan A, Kwan P, et al. Altered metabolic pathways in a transgenic mouse model suggest mechanistic role of amyloid precursor protein overexpression in Alzheimer's disease. *Metabolomics*. 2021;17(5). doi:10.1007/s11306-021-01793-4.
39. Maria K, Luke W, Belinda B, Erickson Kirk I, Elaine H. Associations of the lipidome with ageing, cognitive decline and exercise behaviours. *Metabolites*. 2022;12(9):undefined. doi:10.3390/metabo12090822
40. Han B, Wang JH, Geng Y, Han B, Wang JH, Geng Y. Chronic stress contributes to cognitive dysfunction and hippocampal metabolic abnormalities in APP/PS1 mice. *Cell Physiol Biochem*. 2017;41(5):1766–1776. doi:10.1159/000471869
41. Fonta C, Salles J-P. Salles JP,Neuromuscular features of hypophosphatasia. *Arch Pediatr*. 2017;24(5):5S85–5S88. doi:10.1016/S0929-693X(18)30021-6
42. Fanton S, Menezes J, Krock E, et al. Anti-satellite glia cell IgG antibodies in fibromyalgia patients are related to symptom severity and to metabolite concentrations in thalamus and rostral anterior cingulate cortex. *Brain Behav Immun*. 2023;116:114. doi:10.1016/j.bbi.2023.09.003
43. Zhang X, Wu Q, Lu Y, et al. Cerebroprotection by salvianolic acid B after experimental subarachnoid hemorrhage occurs via Nrf2- and SIRT1-dependent pathways. *Free Radic Biol Med*. 2018;124(0):504–516. 10.1016/j.freeradbiomed.2018.06.035